A 200.2-mW Wireless Power Transfer System with Hybrid SC-/RC-LSK and Triple Regulated Outputs Achieving 66.1% E2E Efficiency

Tianqi Lu, Sijun Du
Department of Microelectronics, Delft University of Technology, Delft, The Netherlands

***Abstract*—This paper presents a 6.78-MHz wireless power transfer (WPT) system for implantable biomedical devices. The receiver (RX) features a compact single-stage triple-output rectifier that delivers three regulated DC outputs (1 V, 2 V, and 3 V) using only two power transistors and two buffer capacitors. A novel load-shift-keying (LSK) technique, hybridizing the short-circuit (SC) LSK and resistive-circuit (RC) LSK, is proposed, achieving low-loss power-data backscattering and fully integrated global power regulation between the RX and transmitter (TX) chips. TX and RX chips were designed and fabricated in a 180-nm BCD process. Measurement results show that the system provides three regulated DC outputs at 1 V, 2 V, and 3 V, respectively, with unnoticeable cross-regulations and load transients. Supplied by a 3.3-V input at TX, it achieves 200.2 mW peak output power, 66.1% peak end-to-end (E2E) power efficiency, and up to 27.3% E2E-efficiency enhancement thanks to global power regulation.**

***Index Terms*—Wireless power transfer (WPT), biomedical implantable devices, triple-output regulation, hybrid load-shift-keying (LSK) backscattering, global power regulation.**

I. Introduction

Wireless power transfer (WPT) is a promising technology for implantable medical devices (IMDs), offering consistent and non-invasive power delivery. As shown in Fig. 1(top), conventional systems typically employ a multi-stage receiver (RX) and an always-on transmitter (TX), which result in low power efficiency and a large RX footprint. Such architectures are unsuitable for advanced IMDs that demand multiple power rails. A recent work [1] presents a single-stage triple-output (SSTO) regulating RX, as depicted in Fig. 1(bottom). While this design supports multiple outputs, it requires eight power transistors (PTs) and an always-on TX, which compromises overall system efficiency.

Meanwhile, global power control techniques have been explored to dynamically regulate the TX power and enhance end-to-end (E2E) efficiency. However, most reported solutions are limited to single-output regulation [2]–[4]. In addition, fully integrated power-data backscattering is highly desirable in wirelessly powered IMDs to minimize the RX volume. This is typically achieved using short-circuit (SC) load-shift-keying (LSK). Nevertheless, SC-LSK incurs significant resonance loss at the TX during uplink data demodulation, as it consumes additional TX power without contributing useful energy to the RX load.

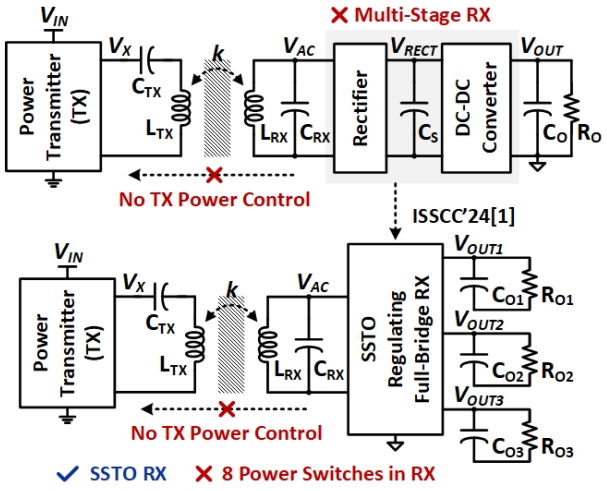

Fig. 1. Conventional wireless power transfer (WPT) system for biomedical devices (top), state-of-the-art triple-output WPT system (bottom).

II. Proposed WPT System

To simultaneously achieve multiple regulated outputs and low-loss global power control, a WPT system is proposed as shown in Fig. 2. Leveraging a voltage doubler topology, the receiver (RX) adopts a stacked-node architecture to generate three regulated outputs from a compact design, as shown in Fig. 2(top). Specifically, V_{O1} and V_{O2} correspond to the voltages across the output capacitors C_{O1} and C_{O2}, respectively, while V_{O3} is formed by stacking V_{O1} and V_{O2}. Although V_{O2} has a shifted ground relative to the other outputs, this facilitates powering circuit blocks operating at different voltage domains within an IMD, with straightforward inter-domain communication enabled via level shifters. Furthermore, by utilizing only two capacitors to deliver three outputs, the design significantly reduces the RX footprint—an essential advantage for space-constrained miniature IMDs.

To further enhance transmitter (TX) efficiency, the proposed system introduces a hybrid global power regulation scheme based on hysteresis control. Conventional hysteresis methods rely solely on short-circuit (SC) load-shift-keying (LSK) at the RX to toggle the TX [3], which results in substantial energy waste at the TX during shutdown transitions, as de-

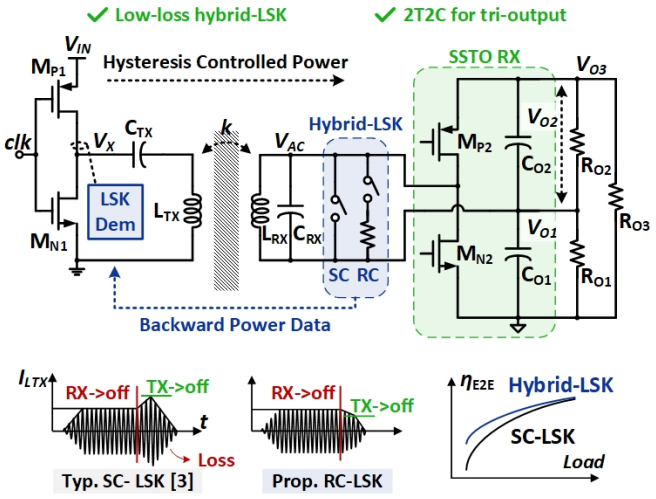

Fig. 2. Proposed WPT system with single-stage triple-output rectifier RX and fully integrated hybrid-LSK backscattering for global TX power regulation.

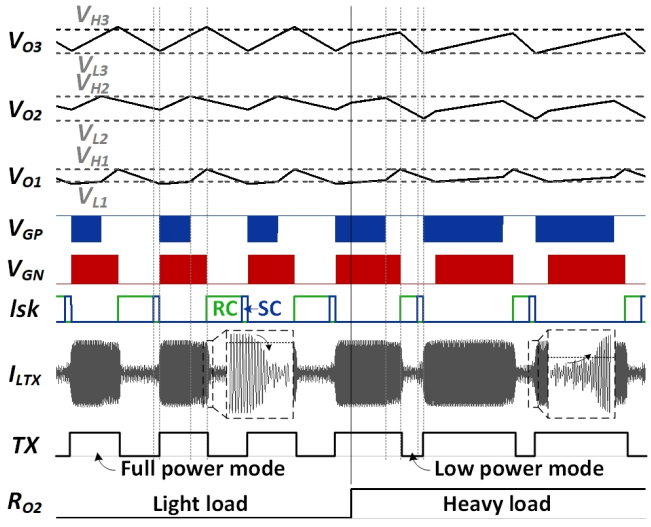

Fig. 3. Operational principle of the proposed WPT system achieving triple-output regulation under R_{O2} load transient.

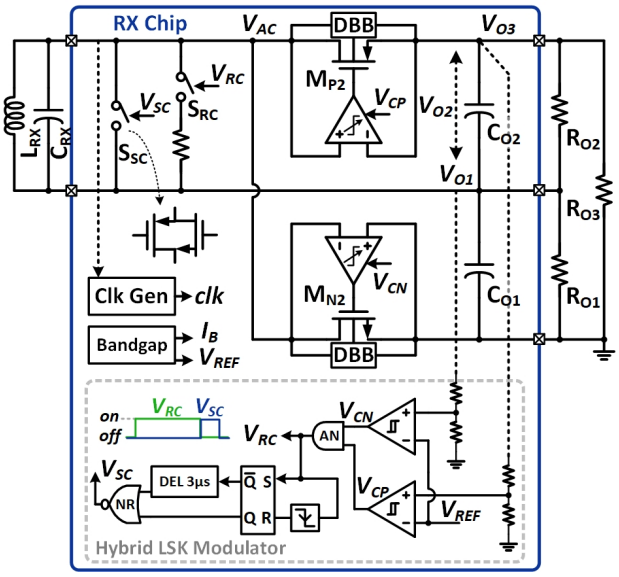

Fig. 4. System diagram of the single-stage triple-output RX with hybrid-LSK modulation.

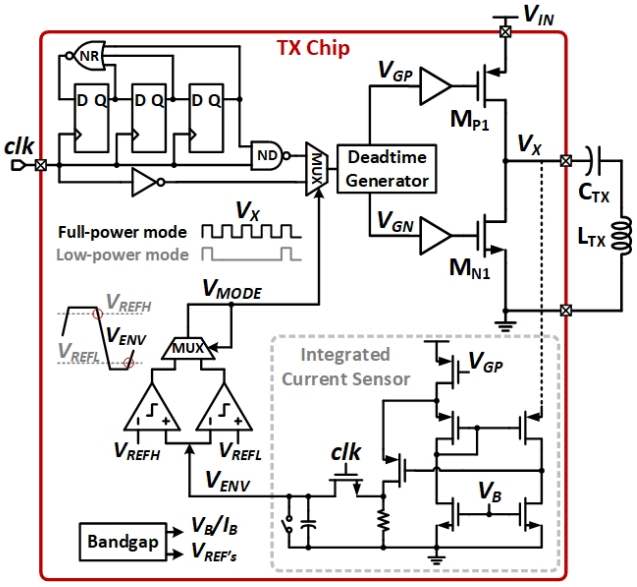

Fig. 5. System diagram of the class-D TX with global hysteresis power regulation based on hybrid-LSK demodulation.

picted in Fig. 2(bottom). To overcome this limitation, this work proposes a fully integrated hybrid LSK technique that synergistically combines SC-LSK with resistive-circuit (RC) LSK. In the proposed scheme, SC-LSK reliably activates the TX, while the RC-LSK deactivates the TX by augmenting the RX resonance and thereby reducing the TX's residual energy consumption during turn-off. This hybrid approach minimizes transition losses, effectively boosting both TX and end-to-end (E2E) system efficiency.

Fig. 3 shows the operation waveform. The RX outputs are regulated by holding the voltages across C_{O1} and C_{O2} within independent hysteresis windows. Since C_{O1} and C_{O2} are respectively charged by M_{N1} and M_{P1}, their voltages can be independently regulated [5]. When all three outputs do not require power input, the RX sends an RC-LSK signal to reduce TX power to a very low level by pulse-skipping control. If any output demands power, an SC-LSK signal is sent to the TX to resume the TX power to full scale.

III. Circuit Implementations

Fig. 4 illustrates the RX architecture. The hybrid-LSK switches, S_{SC} and S_{RC}, are realized as transmission gates to enable efficient modulation between short-circuit and resistive-circuit modes. Two PTs, M_{N1} and M_{P1}, are equipped with adaptive gate biases and dynamic body biases (DBB) to ensure robust turn-off characteristics and reliable output regulation [5]. Furthermore, their active-diode operation is enhanced by adaptive delay compensation, enabling near-zero voltage switching and minimizing conduction losses. The hybrid-LSK

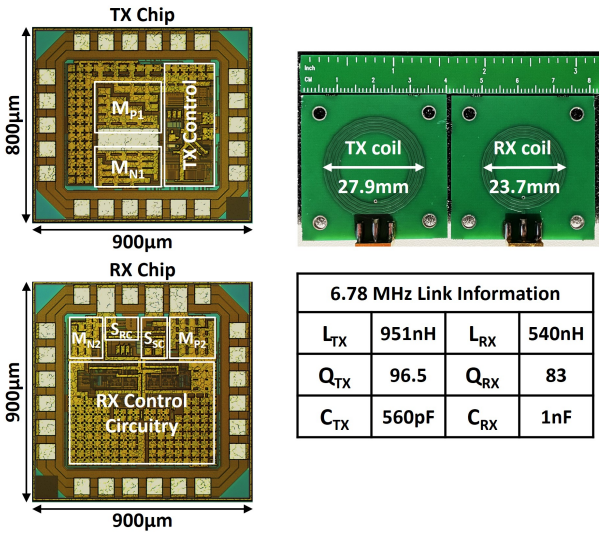

6.78 MHz Link Information			
L_{TX}	951nH	L_{RX}	540nH
Q_{TX}	96.5	Q_{RX}	83
C_{TX}	560pF	C_{RX}	1nF

Fig. 6. Chip photos of the proposed TX and RX chips, and the 6.78-MHz inductive link information.

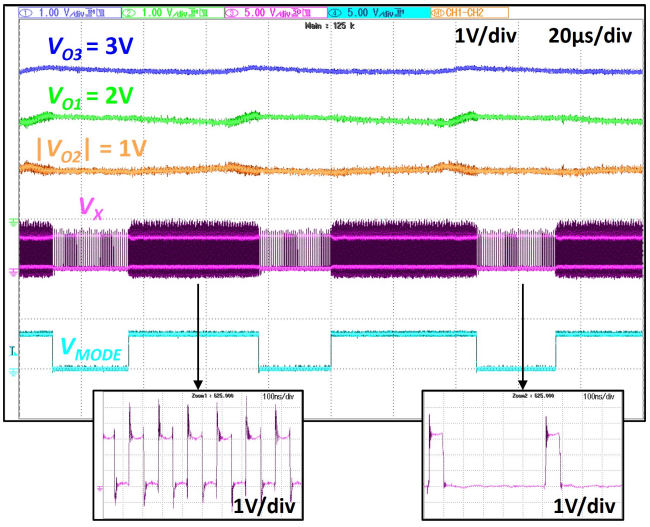

Fig. 7. Measured steady-state waveform of the proposed WPT system at V_{IN} = 3.3 V, D_{COIL} = 1.5 cm, and R_{O1} = R_{O2} = R_{O3} = 700 Ω.

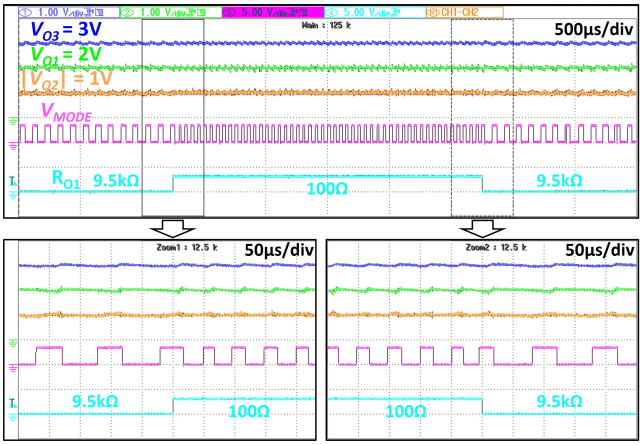

Fig. 8. Measured load-transient waveform of the proposed WPT system at V_{IN} = 3.3 V, D_{COIL} = 1.5 cm, and R_{O2} = R_{O3} = 1 kΩ.

modulator generates the RC-LSK and SC-LSK control pulses (V_{RC} and V_{SC}), which are determined based on the control signals V_{CN} and V_{CP} derived from hysteresis comparators that monitor the output voltages. This architecture enables fully integrated, low-loss backscattering control within the RX.

Fig. 5 presents the TX circuit architecture. A class-D power amplifier energizes the TX resonance tank, while an integrated current sensor monitors the high-side current, producing an envelope signal that reflects the resonant amplitude. By detecting the rising and falling edges of this current envelope, the TX accurately demodulates the hybrid-LSK signals from the RX. To reduce power consumption during idle or light-load conditions, the TX enters a low-power mode by skipping three out of every four resonant positive cycles, effectively achieving a 75% power reduction relative to full-power operation. This pulse-skipping strategy significantly improves transmitter efficiency without compromising responsiveness to RX demands.

IV. Measurement Results

Fig. 6 exhibits the TX and RX chip photos and the 6.78-MHz inductive link specifications. The TX and RX chips occupy 0.72 mm^2 and 0.81 mm^2, respectively, including pad rings. Fig. 7 shows the measured steady-state waveform at V_{IN} = 3.3 V, coil separation distance D_{COIL} = 1.5 cm, and loads R_{O1} = R_{O2} = R_{O3} = 700 Ω. It's observed that V_{O1}, V_{O2}, and V_{O3} are regulated at 2 V, 1 V, and 3 V, respectively. These voltage levels can be adjusted depending on applications. With the hybrid-LSK modem, the TX switches between full-power and low-power modes with a duty ratio.

Fig. 8, as measured load-transient waveform, shows unnoticeable cross-regulations and load transients at outputs when R_{O1} varies between 100 Ω and 9.5 kΩ. Fig. 9 displays the measured hybrid-LSK demodulation waveform. After the RX triggers RC-LSK (V_{RC}'s rising edge), the amplitude of the TX coil current, I_{LTX}, decreases. This change in I_{LTX} is detected to turn the TX to low-power mode. When the RX requests power, a 3-μs SC-LSK pulse (V_{SC}) is generated. This results in an amplitude increase in I_{LTX}, which is detected to turn TX into full-power mode.

Fig. 10 shows the measured E2E (from TX input to RX output) power efficiency at D_{COIL} of 0.5 cm and 1.5 cm. A peak E2E efficiency is obtained at 66.1% when D_{COIL} = 0.5 cm. The maximum output power reaches 200.2 mW at D_{COIL} = 1.5 cm. Due to the frequency-splitting effect, the maximum output power is not achieved under the stronger coupling condition. Fig. 11 shows that up to 27.3% E2E efficiency improvement is achieved with the proposed hybrid-LSK-based global power control, which accordingly results in 2.2× input power reduction at TX.

Table I compares this work with recently reported WPT systems for IMDs [6], [7]. Thanks to the proposed triple-output architecture and the low-loss hybrid-LSK backscattering scheme, this design achieves a reduction in power component count and die area, while delivering competitive output power and superior E2E efficiency. Notably, the system main-

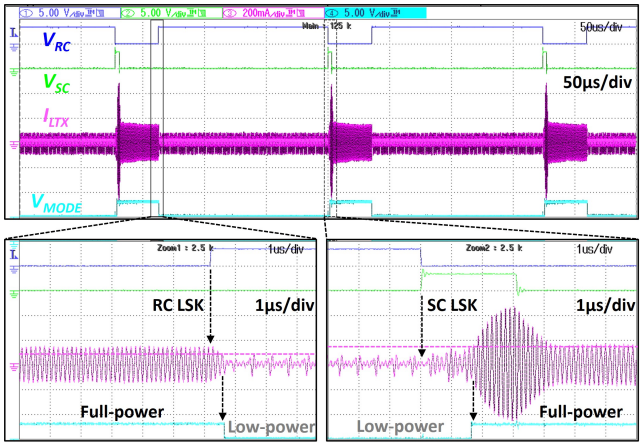

Fig. 9. Measured hybrid-LSK demodulation waveform of the proposed WPT system at V_{IN} = 3.3 V, D_{COIL} = 1 cm, and R_{O1} = R_{O2} = R_{O3} = 1 kΩ.

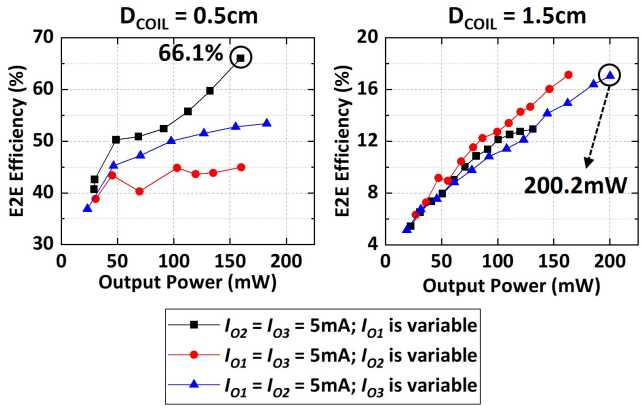

Fig. 10. Measured end-to-end (E2E) power efficiency of the proposed WPT system versus output power at V_{IN} = 3.3 V. I_{O1}, I_{O2}, and I_{O3} are the output currents flowing through R_{O1}, R_{O2}, and R_{O3}, respectively.

tains state-of-the-art output power levels with fewer power transistors and a more compact footprint, making it particularly well-suited for space-constrained biomedical implants.

V. Conclusions

This paper presents a 6.78-MHz wireless power transfer (WPT) system for bio-implant applications. The proposed system features a hybrid load-shift-keying (LSK) power-data backscattering technique that minimizes transmitter resonance energy loss, thereby enhancing end-to-end (E2E) power efficiency. A single-stage rectifier at the receiver simultaneously delivers three regulated DC outputs (1 V, 2 V, and 3 V) with negligible cross-regulation and fast transient responses. Experimental results validate peak output power of 200.2 mW, achieving up to 66.1% peak E2E efficiency and demonstrating a maximum 27.3% E2E-efficiency improvement compared to unregulated WPT methods.

Acknowledgment

The authors would like to thank Makoto Takamiya from the University of Tokyo, Japan, for fruitful discussions and valuable suggestions.

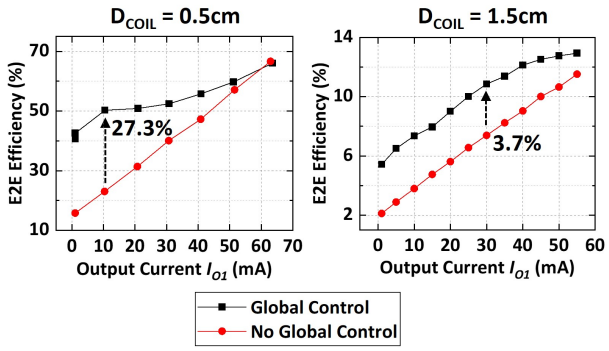

Fig. 11. Measured E2E power efficiency versus output current, I_{O1}, with or without global power regulation at V_{IN} = 3.3 V and I_{O2} = I_{O3} = 5 mA.

TABLE I
Comparison with state-of-the-art WPT systems.

	JSSC'18[2]	ISSCC'21[3]	TCASI'23[6]	VLSI'24[7]	This work
Technology (nm)	65 CMOS	180 CMOS	180 CMOS	180 CMOS	**180 BCD**
Frequency (MHz)	13.56	6.78	6.78	6.78	**6.78**
Die Area (mm²)	TX 1.44; RX 1.44	TX 0.98; RX 1.3	TX 0.98; RX 2.7	RX 1.72	**TX 0.72; RX 0.81**
Global Power Regulation	Constant Off-Time	Hysteresis	Hysteresis	N/A	**Hysteresis**
Wireless Power Data Link	SC LSK	SC LSK	SC LSK	Harmonic comm.	**Hybrid RC/SC LSK**
TX V_{IN} (V)	2.5	1.8	1.8	5*	**3.3**
RX V_O (V)	1.2-2.5	1.2-1.8	1.8, 3	3	**1, 2, 3**
# of RX V_O	1	1	2	1	**3**
RX Power Component	4 PT; 1 C_O	4 PT; 1 C_O	6 PT; 2 C_O	6 PT; 2 C_O	**2 PT; 2 C_O**
Output power (mW)	49.4	32	7	82	**200.2**
E2E Efficiency	69%	61.9%	31.3%	52.6%	**66.1%**

*Estimated from paper.

References

[1] H.-S. Lee, K. Eom, and H.-M. Lee, "27.3 a 90.8%-efficiency simo resonant regulating rectifier generating 3 outputs in a half cycle with distributed multi-phase control for wirelessly-powered implantable devices," in *ISSCC*, 2024, pp. 448–450.

[2] C. Huang, T. Kawajiri, and H. Ishikuro, "A 13.56-mhz wireless power transfer system with enhanced load-transient response and efficiency by fully integrated wireless constant-idle-time control for biomedical implants," *IEEE Journal of Solid-State Circuits*, vol. 53, no. 2, pp. 538–551, 2018.

[3] J. Tang, L. Zhao, and C. Huang, "A wireless hysteretic controlled wireless power transfer system with enhanced efficiency and dynamic response for bioimplants," *IEEE Journal of Solid-State Circuits*, pp. 1–12, 2022.

[4] T. Lu and S. Du, "A coupling-adaptive wireless power transfer system with voltage-/current-mode receiver and global digital-pwm regulation," *IEEE Journal of Solid-State Circuits*, pp. 1–13, 2024.

[5] T. Lu, K. A. A. Makinwa, and S. Du, "A single-stage dual-output regulating voltage doubler for wireless power transfer," *IEEE Journal of Solid-State Circuits*, pp. 1–12, 2024.

[6] D.-H. Yao, T.-N. Liu, M. Takamiya, and P.-H. Chen, "A 6.78-mhz wireless power transfer system with dual-output resonant current-mode regulating rectifier and transmission power regulation," *IEEE Transactions on Circuits and Systems I: Regular Papers*, vol. 70, no. 12, 2023.

[7] Q. Zhuang, J. Sun, X. Zhang, B. Li, Y. Shi, and H. Qiu, "A 6.78 mhz wireless power and data transfer system achieving simultaneous 52.6% end-to-end efficiency and 4.0 mb/s forward data delivery with interference-free rectifier," in *2024 IEEE Symposium on VLSI Technology and Circuits (VLSI Technology and Circuits)*, 2024, pp. 1–2.